

## Collisionless Dynamo

Robert G. Kleva

*Institute for Plasma Research, University of Maryland, College Park, Maryland 20742*

(Received 18 February 1994)

Electron inertia is shown to dramatically impact the generation of a magnetic field by a flowing collisionless plasma. The rate at which magnetic field energy is created by the flow remains large as the magnetic Reynolds number  $R_m \rightarrow \infty$ , for both chaotic and nonchaotic flows. Importantly, a continuous nonchaotic laminar flow generates a magnetic field in a collisionless (zero collisional diffusion) plasma because of electron inertia. The magnetic field generated lies in a series of flux bundles with a scale size given by the collisionless electron skin depth.

PACS numbers: 95.30.Qd, 51.60.+q, 52.30.-q

Magnetic fields are ubiquitous in the Universe. The origin of these magnetic fields has been a fundamental subject of inquiry for many years. It is well known that magnetic fields can be generated by the motion of a conducting fluid. This process is described by Faraday's law for the time evolution of the magnetic field  $\mathbf{B}$ ,  $\partial\mathbf{B}/\partial t = -c\nabla \times \mathbf{E}$ , together with Ohm's law for the electric field  $\mathbf{E}$ . In the resistive magnetohydrodynamics (MHD) approximation, Ohm's law is given by  $\mathbf{E} + \mathbf{V} \times \mathbf{B}/c = \eta\mathbf{J}$ , where the current  $\mathbf{J} = (c/4\pi)\nabla \times \mathbf{B}$ ,  $\mathbf{V}(\mathbf{x}, t)$  is the velocity of the conducting fluid, and  $\eta$  is the resistivity. Let us write the MHD equations in normalized units by making the following replacements:  $\mathbf{V}/V_0 \rightarrow \mathbf{V}$  where  $V_0$  is the characteristic magnitude of  $\mathbf{V}$ ,  $\mathbf{x}/L \rightarrow \mathbf{x}$  where  $L$  is the scale length characteristic of  $\mathbf{V}$ , and  $V_0 t/L \rightarrow t$ . Then, the time rate of change of the magnetic field in resistive MHD is given by the induction equation

$$\partial\mathbf{B}/\partial t = \nabla \cdot (\mathbf{B}\mathbf{V} - \mathbf{V}\mathbf{B}) + R_m^{-1}\nabla^2\mathbf{B}, \quad (1)$$

where the magnetic Reynolds number  $R_m = 4\pi LV_0/\eta c^2$  and the collisional diffusion is given by  $R_m^{-1}$ . The induction equation (1) is linear in  $\mathbf{B}$ . The generation of a magnetic field, which grows exponentially in time, by a specified flow  $\mathbf{V}$  is called a kinematic dynamo.

Classically, the resistance of a conducting fluid to an electric field is determined by the binary Coulomb collisions between the ions and the current carrying electrons. Since astrophysical plasmas are nearly collisionless, the resistivity  $\eta$  is very small and the magnetic Reynolds number is very large ( $R_m > 10^8$ ). Therefore, the sensitivity of the rate  $\gamma$  at which the magnetic field is generated by a dynamo to the magnitude of  $R_m$  is very important. The dynamo is "fast" if  $\gamma$  remains nonzero as  $R_m \rightarrow \infty$ . Conversely, if  $\gamma \rightarrow 0$  as  $R_m \rightarrow \infty$ , then the dynamo is "slow." Slow dynamos are not believed to be likely candidates for the effective generation of magnetic fields in astrophysical plasmas where  $R_m$  is very large. It is widely believed that only chaotic flows can generate a fast dynamo [1-4], and, therefore, that only chaotic flows are relevant for astrophysical dynamos.

Many investigations have demonstrated that magnetic fields can be generated by a specified flow [1-16]. One particularly well-studied class of flows are the *ABC* flows [17] with velocity components  $V_x = A \sin z + C \cos y$ ,  $V_y = B \sin x + A \cos z$ , and  $V_z = C \sin y + B \cos x$ . The *ABC* flows are periodic in space with period  $2\pi$  in  $x$ ,  $y$ , and  $z$ , time-independent, incompressible ( $\nabla \cdot \mathbf{V} = 0$ ), and the vorticity  $\boldsymbol{\omega} = \nabla \times \mathbf{V} = \mathbf{V}$ . If one of the parameters  $A$ ,  $B$ , or  $C$  is zero, then the flow is integrable [17]. When all of the parameters  $A$ ,  $B$ , and  $C$  are nonzero (for example,  $A = B = C = 1$ ), then chaotic streamlines exist in a portion of space [17].

Magnetic field generation by a chaotic *ABC* flow in the resistive MHD approximation has been investigated numerically by Galloway and Frisch [2]. They found that the growth rate of the magnetic field does not decrease as the Reynolds number increases to  $R_m = 550$ , the largest value of  $R_m$  that they investigated. The magnetic field generated is concentrated in narrow structures centered on the stagnation points of the flow. The width of these structures decreases as  $R_m$  increases, scaling as  $R_m^{-1/2}$ . Finn and Ott [11] studied a chaotic map, related to the *ABC* flows, in the zero-resistivity limit ( $R_m = \infty$ ). They found that the magnetic flux concentrates on a fractal and that the magnetic field exhibits arbitrarily fine-scaled oscillations between the parallel and antiparallel directions.

Magnetic field generation by a nonchaotic *ABC* flow in the resistive MHD approximation has been studied analytically by Soward [7]. The growth rate decreases as  $R_m$  increases, although the decrease is very small, the growth rate scaling as  $\ln(\ln R_m)/\ln R_m$ . In a collisionless plasma ( $R_m = \infty$ ), a nonchaotic *ABC* flow cannot generate a magnetic field. As in the case of a chaotic flow, the magnetic field is concentrated in narrow structures whose width decreases as  $R_m$  increases, the width scaling as  $R_m^{-1/2}$ .

Therefore, in the resistive MHD approximation, for dynamos driven by both chaotic and continuous nonchaotic flows, the magnetic field generated lies in narrow structures whose width decreases to zero as  $R_m \rightarrow \infty$ . In the

zero-resistivity collisionless limit, magnetic field energy can only be generated by chaotic flows, and the field generated is concentrated on a fractal. A continuous, non-chaotic flow cannot generate a magnetic field in a collisionless plasma. The singular nature of the magnetic field in the  $R_m \rightarrow \infty$  limit suggests that nonideal effects other than collisionality in Ohm's law, which are neglected in resistive MHD, may be important in nearly collisionless plasmas. When the collisional diffusion is zero, the ideal MHD constraint tying the magnetic field lines to the flow is still broken by the finite (nonzero) electron mass.

In this Letter I demonstrate that electron inertia dramatically alters the kinematic dynamo in collisionless plasmas. In contradiction to the resistive MHD prediction, continuous nonchaotic laminar flows generate magnetic fields in collisionless plasmas (where the collisional diffusion  $R_m^{-1}$  is zero) because of electron inertia. Thus, the distinction made between dynamos generated by chaotic and nonchaotic flows in resistive MHD becomes meaningless with electron inertia. The rate at which magnetic field energy is generated at large  $R_m$  can be greatly enhanced by electron inertia for chaotic as well as non-chaotic flows. The magnetic field generated by a chaotic flow in a collisionless plasma is not fractal in structure. Instead, the scale size of the field generated is given by the electron skin depth.

Consider the general form of Ohm's law [18],

$$\mathbf{E} + \frac{\mathbf{V} \times \mathbf{B}}{c} - \frac{\mathbf{J} \times \mathbf{B}}{nec} + \frac{\nabla P_e}{ne} = \frac{m_e}{ne^2} \left[ \frac{\partial \mathbf{J}}{\partial t} + \nabla \cdot (\mathbf{V}\mathbf{J} + \mathbf{J}\mathbf{V}) \right] + \eta \mathbf{J}, \quad (2)$$

which includes the effect of the nonzero electron mass  $m_e$  and the force caused by gradients in the electron pressure,  $P_e$ , in addition to collisions, and where  $n$  is the number density of electrons. Insertion of the generalized Ohm's law in Eq. (2) into Faraday's law yields the generalized induction equation

$$\frac{\partial}{\partial t} (\mathbf{B} - d_e^2 \nabla^2 \mathbf{B}) = \nabla \cdot (\mathbf{B}\mathbf{V} - \mathbf{V}\mathbf{B}) - d_e^2 \nabla \times [\nabla \cdot (\mathbf{V}\mathbf{J} + \mathbf{J}\mathbf{V})] + R_m^{-1} \nabla^2 \mathbf{B}, \quad (3)$$

where the electron collisionless skin depth  $d_e = c/\omega_{pe}$ , with the electron plasma frequency  $\omega_{pe} = (4\pi ne^2/m_e)^{1/2}$ , and the current  $\mathbf{J} = \nabla \times \mathbf{B}$ . The nonzero electron mass  $m_e$  introduces the scale length  $d_e$  into the dynamo problem. Equation (3) is written in the normalized units given before Eq. (1). Thus, the skin depth  $d_e$  in Eq. (3) is normalized to the scale length  $L$  of the flow. Gradients in the electron pressure do not contribute to the dynamo. Consistent with the neglect of the nonlinear  $\mathbf{J} \times \mathbf{B}$  force in the fluid momentum equation in the kinematic dynamo problem, the nonlinear  $\mathbf{J} \times \mathbf{B}$  force in the generalized

Ohm's law (2) has been neglected in the derivation of Eq. (3). As a result, the generalized induction equation (3) is linear in  $\mathbf{B}$ .

The induction equation (3) is solved on a triply periodic Cartesian grid, with period  $L = 2\pi$  in  $x$ ,  $y$ , and  $z$ , and with the flow velocity  $\mathbf{V}$  given by an  $ABC$  flow. Spatial derivatives are evaluated to fourth order in the grid spacing  $\Delta$  [19] while time stepping is second order accurate in the time step  $\Delta t$  with a leapfrog trapezoidal scheme [20]. The number of grid points retained is varied to ensure that the results are not sensitive to this number. The Laplacian  $\nabla^2$  operator is inverted by means of a three-dimensional fast Fourier transform.

Let us define the total magnetic energy  $\langle B^2(t) \rangle$  at time  $t$  by

$$\langle B^2(t) \rangle = \int_0^{2\pi} dx \int_0^{2\pi} dy \int_0^{2\pi} dz [B_x^2(x, y, z, t) + B_y^2(x, y, z, t) + B_z^2(x, y, z, t)].$$

From an initial perturbation, the magnetic field evolves into a steady state in which  $\langle B^2(t) \rangle$  increases exponentially in time:  $\langle B^2(t) \rangle = \langle B^2(t_0) \rangle \exp[2\gamma(t - t_0)]$ , where  $\gamma$  is the growth rate.

Figure 1 is a plot of  $\gamma$  as a function of the magnetic Reynolds number  $R_m$  for a continuous, nonchaotic,  $ABC$  flow with  $A = B = 1$  and  $C = 0$  (the flow is independent of the  $y$  coordinate). The crosses are the results from simulations using the resistive MHD Ohm's law ( $d_e = 0$ ), while the results obtained using the generalized Ohm's law including electron inertia ( $d_e = 0.2$ ) are given by the circles. The point at  $R_m = \infty$  is for a plasma with zero collisional diffusion. In the resistive MHD approximation, the growth rate  $\gamma$  slowly decreases towards zero as  $R_m$  increases. Electron inertia dramatically alters this

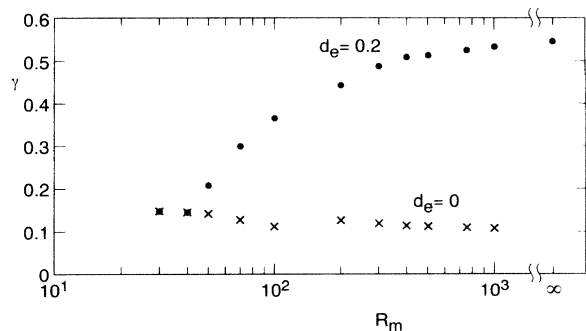


FIG. 1. Magnetic dynamo with electron inertia. The growth rate  $\gamma$  of the magnetic field generated by a nonchaotic  $ABC$  flow ( $A = B = 1$ ,  $C = 0$ ) is plotted as a function of the magnetic Reynolds number  $R_m$ . The crosses are the results from simulations using the resistive MHD equations ( $d_e = 0$ ), while the circles are the results from simulations which include the effect of electron inertia ( $d_e = 0.2$ ).

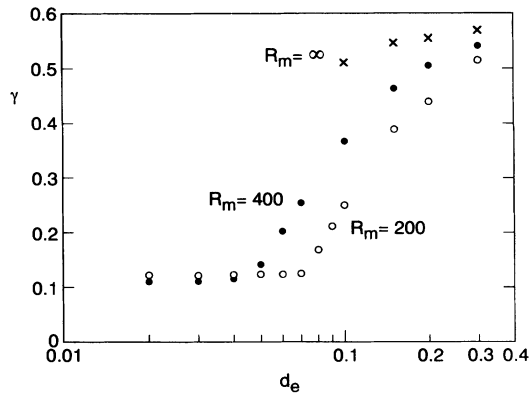


FIG. 2. Nonchaotic dynamo. The growth rate  $\gamma$  of the magnetic field generated by a nonchaotic  $ABC$  flow ( $A = B = 1, C = 0$ ) is plotted as a function of the electron skin depth  $d_e$  for three different values of the Reynolds number:  $R_m = 200$  (open circles), 400 (solid circles), and  $\infty$  (crosses).

picture. At very small  $R_m$ , the effect of electron inertia is negligible. However, as  $R_m$  increases beyond 40, the growth rate of the magnetic field becomes larger than the resistive MHD rate. Furthermore, unlike resistive MHD where  $\gamma$  slowly decreases as  $R_m$  increases, with electron inertia  $\gamma$  actually increases as  $R_m$  increases and the plasma becomes less collisional. When  $R_m = 1000$ , the growth rate with  $d_e = 0.2$  is more than 5 times as large as the growth rate in resistive MHD ( $d_e = 0$ ). Importantly, the growth rate generated by a continuous, nonchaotic  $ABC$  flow remains nonzero and large even in a collisionless ( $R_m = \infty$ ) plasma, when the physics of electron inertia is retained. This is in marked contrast to resistive MHD where a continuous, nonchaotic flow is incapable of generating magnetic field in a collisionless plasma.

Figure 2 is a plot of  $\gamma$  as a function of the electron skin depth  $d_e$  for a continuous, nonchaotic  $ABC$  flow with  $A = B = 1$  and  $C = 0$ , and for three different values of  $R_m$ ;  $R_m = 200, 400, \infty$ , where the points labeled by " $R_m = \infty$ " are for a plasma with zero collisional diffusion. When the plasma is very collisional ( $R_m = 200$ ) and  $d_e$  is very small, one recovers the resistive MHD result. However, when  $d_e$  exceeds a critical value  $d_{crit}$  of roughly  $7 \times 10^{-2}$  then  $\gamma$  becomes larger than the resistive MHD prediction, increasing as  $d_e$  increases further. The results for  $R_m = 400$  are qualitatively the same as those for  $R_m = 200$ . However, the critical value of  $d_e$ , beyond which  $\gamma$  exceeds the resistive MHD prediction, is roughly  $d_{crit} \cong 4 \times 10^{-2}$ , smaller than the critical value in the more collisional plasma with  $R_m = 200$ . Thus, as the plasma becomes less collisional and  $R_m$  becomes very large, the effect of the nonzero electron inertia becomes increasingly important. In a collisionless plasma ( $R_m = \infty$ ), the growth rate of the magnetic field remains nonzero and large because of electron inertia.

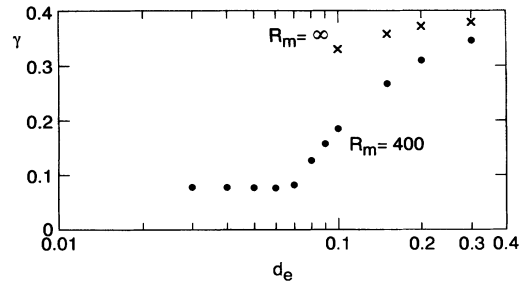


FIG. 3. Chaotic dynamo. The growth rate  $\gamma$  of the magnetic field generated by a chaotic  $ABC$  flow ( $A = B = C = 1$ ) is plotted as a function of the electron skin depth  $d_e$  for two different values of the Reynolds number:  $R_m = 400$  (circles) and  $\infty$  (crosses).

Suppose that the inverse scaling of  $d_{crit}$  with  $R_m$  is given by a power law,  $d_{crit}/L = AR_m^{-\alpha}$ , where the power  $\alpha$  and the proportionality constant  $A$  are positive numbers and  $L = 2\pi$  is the scale size of the flow. From the results for  $d_{crit}$  at  $R_m = 200$  and at  $R_m = 400$  one finds that the power  $\alpha \cong 0.8$  and the proportionality constant  $A \cong 0.8$ . One might expect that electron inertia will be important when  $d_e$  exceeds the width of the narrow flux bundles generated by collisions in resistive MHD scales as  $R_m^{-1/2}$ , the exponent  $\alpha$  in the scaling law for  $d_{crit}$  would be  $\frac{1}{2}$ . Given the uncertainty in the calculation of  $\alpha$  from these two data points, a square root scaling is not inconsistent with the results.

Figure 3 is a plot of  $\gamma$  as a function of  $d_e$  for a chaotic  $ABC$  flow with  $A = B = C = 1$ , and for two values of  $R_m$ :  $R_m = 400, \infty$ , where the points labeled by " $R_m = \infty$ " are for a plasma with zero collisional diffusion. The results for the chaotic flow are similar to those for the continuous, nonchaotic flow shown in Fig. 2. When the plasma is very collisional ( $R_m = 400$ ) and  $d_e$  is small, one recovers the resistive MHD result. However, when  $d_e$  exceeds a critical value of roughly  $d_{crit} \cong 7 \times 10^{-2}$  then  $\gamma$  becomes larger than the resistive MHD prediction, increasing as  $d_e$  increases further. In a collisionless plasma, the growth rate of the magnetic field remains large because of electron inertia.

Figure 4 is a plot of the surface  $B^2 = \frac{1}{3}B_{max}^2$  in the periodic box  $0 \leq x, y, z \leq 2\pi$  for the magnetic field generated by the (a) chaotic and (b) nonchaotic flow in a collisionless ( $R_m = \infty$ ) plasma with  $d_e = 0.2$  where  $B_{max}^2$  is the maximum value of  $B^2$  in the box. In the resistive MHD approximation, the magnetic field generated by the chaotic flow would have a fractal structure, but with electron inertia the scale size of the flux bundles is nonzero and of the order of  $d_e$ . The nonchaotic flow would not generate a magnetic field in a collisionless plasma in the absence of electron inertia.

In conclusion, electron inertia has been shown to dramatically alter the kinematic dynamo in collisionless

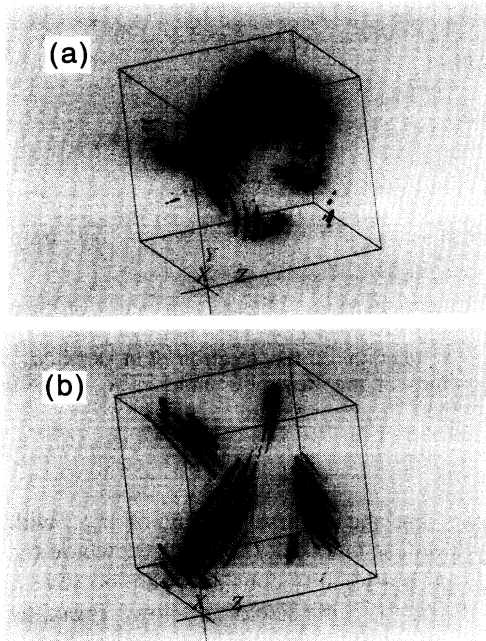


FIG. 4. Flux bundles. A surface of constant  $B^2 = \frac{1}{3}B_{\max}^2$  generated by a (a) chaotic and (b) nonchaotic ABC flow in a collisionless plasma (zero dissipation) is plotted in the box  $0 \leq x \leq 2\pi$ ,  $0 \leq y \leq 2\pi$ ,  $0 \leq z \leq 2\pi$ , where  $B_{\max}^2$  is the maximum value of  $B^2$ .

plasmas. Unlike the resistive MHD result, the rate at which magnetic field energy is created by the flow remains large as  $R_m \rightarrow \infty$ , for both chaotic and nonchaotic flows. When the collisional diffusion  $R_m^{-1}$  is zero, the ideal MHD constraint tying the magnetic field lines to the flow is still broken by the finite (nonzero) electron mass. As an important consequence, a continuous nonchaotic

laminar flow generates a magnetic field in a collisionless plasma because of electron inertia.

- 
- [1] V. I. Arnol'd, Ya. B. Zel'dovich, A. A. Ruzmaikin, and D. D. Sokolov, *Sov. Phys. JETP* **54**, 1083 (1981).
  - [2] D. Galloway and U. Frisch, *Geophys. Astrophys. Fluid Dyn.* **36**, 53 (1986).
  - [3] Y. T. Lau and J. M. Finn, *Phys. Fluids B* **5**, 365 (1993).
  - [4] S. Childress, *Phys. Earth Planet. Int.* **20**, 172 (1979).
  - [5] S. A. Molchanov, A. A. Ruzmaikin, and D. D. Sokolov, *Sov. Phys. Usp.* **28**, 307 (1985).
  - [6] H. K. Moffatt and M. R. E. Proctor, *J. Fluid Mech.* **154**, 493 (1985).
  - [7] A. M. Soward, *J. Fluid Mech.* **180**, 267 (1987).
  - [8] B. J. Bayly and S. Childress, *Phys. Rev. Lett.* **59**, 1573 (1987).
  - [9] F. W. Perkins and E. G. Zweibel, *Phys. Fluids* **30**, 1079 (1987).
  - [10] J. M. Finn and E. Ott, *Phys. Rev. Lett.* **60**, 760 (1988).
  - [11] J. M. Finn and E. Ott, *Phys. Fluids* **31**, 2992 (1988).
  - [12] B. J. Bayly and S. Childress, *Geophys. Astrophys. Fluid Dyn.* **44**, 211 (1988).
  - [13] A. D. Gilbert, *Geophys. Astrophys. Fluid Dyn.* **44**, 241 (1988).
  - [14] J. M. Finn and E. Ott, *Phys. Fluids B* **2**, 916 (1990).
  - [15] A. D. Gilbert and S. Childress, *Phys. Rev. Lett.* **65**, 2133 (1990).
  - [16] J. M. Finn, J. D. Hanson, I. Kan, and E. Ott, *Phys. Fluids B* **3**, 1250 (1991).
  - [17] T. Dombre, U. Frisch, J. M. Greene, M. Henon, A. Mehr, and A. M. Soward, *J. Fluid Mech.* **167**, 353 (1986).
  - [18] N. A. Krall and A. W. Trivelpiece, *Principles of Plasma Physics* (McGraw-Hill, New York, 1973), p. 91.
  - [19] S. T. Zalesak, *J. Comput. Phys.* **40**, 497 (1981).
  - [20] Y. Kuribara, *Mon. Weather Rev.* **93**, 13 (1965).

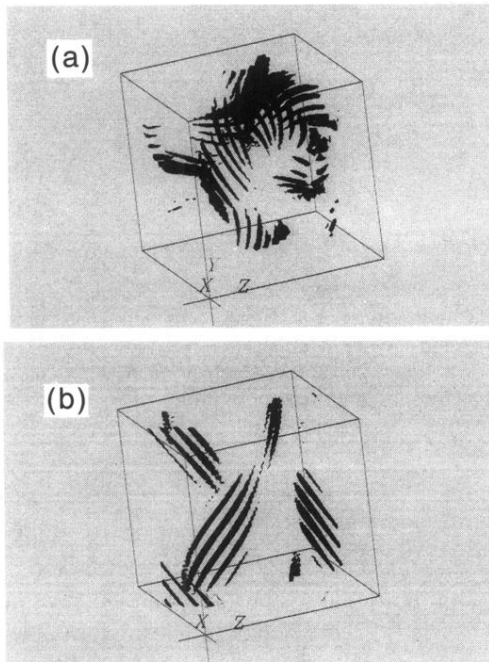


FIG. 4. Flux bundles. A surface of constant  $B^2 = \frac{1}{3}B_{\max}^2$  generated by a (a) chaotic and (b) nonchaotic  $ABC$  flow in a collisionless plasma (zero dissipation) is plotted in the box  $0 \leq x \leq 2\pi$ ,  $0 \leq y \leq 2\pi$ ,  $0 \leq z \leq 2\pi$ , where  $B_{\max}^2$  is the maximum value of  $B^2$ .